Path dependence of structural relaxation of elastomeric glasses

C.-L. Tang*, K. Vijayan and K. D. Pae
High Pressure Materials Research Laboratory, Department of Mechanics and Materials Science, College of Engineering, Rutgers University, Piscataway, NJ 08855-0909, USA
(Received 1 December 1986; accepted 28 July 1987)

A theoretical calculation based on the general solution of a multi-ordering-parameter model is extended to study combined pressure and temperature effects on the relaxation of a polyurethane elastomeric glass (Solithane 113). Distinctly different relaxation behaviours were produced at a point (P,T) when the glasses arrived at that point by different paths, namely along an isobar and along an isotherm. The general solution for the kinetics of a certain path takes the form:

$$\delta(t)=\delta_0\phi(t,t_0)-\int_{t_0}^{t}(\Delta\alpha q-\Delta\beta p)\phi(t,t')\,\mathrm{d}t'$$

where the relaxation time involved in ϕ is an explicit function of P, T, P_f (fictive pressure) and T_f (fictive temperature). The variables T and T_f, and P and P_f are mutually convertible by the relationship $\mathrm{d}\delta=\Delta\beta\mathrm{d}(P-P_f)=\Delta\alpha\mathrm{d}(T_f-T)$, in which both $\Delta\beta$ and $\Delta\alpha$ are functions of P and T. During the ageing of the elastomeric glass, Young's modulus (E) was measured at various intervals of ageing time to monitor the variation of δ, the volumetric measure of departure from equilibrium, related to E by $\delta=A(P,T)[1/E(t)-1/E_\infty(P,T)]$. Ageing behaviour and memory effects caused by combination of pressure and temperature perturbations were investigated to predict the experimental results. Detailed experimental techniques and procedures have been described in earlier papers.

(Keywords: path dependence; physical ageing; relaxation; elastomeric glass; multi-ordering parameter; isobar; isotherm; kinetics of relaxation)

INTRODUCTION

Polymeric glasses may be formed by lowering temperature, increasing pressure or combining both as a result of gradual reduction of the rate of molecular motion. When the rate of cooperative rearrangement of polymer chain segments becomes of the same order of magnitude as the rate of cooling or pressurizing, in other words, the relaxation time τ is comparable to the timescale of observation t, the glass transition of an amorphous polymer occurs. Glasses usually exist in a non-equilibrium state and will relax continuously towards the equilibrium state with a rate depending on the relaxation time. This phenomenon is commonly referred to as physical ageing.

Theoretical considerations based on statistical mechanics[1-6] indicate that the glass transition is a thermodynamic transformation, assuming the freezing-in model of internal parameters[7]. However, owing to the knowledge that ageing of a glass is a purely kinetic process[8,9] which is inherently related to the relaxation time, there seems to be a tendency at present to treat a glass transition as a kinetically controlled process[10,11]. The kinetic aspects of glass transition subject to different kinds of thermal treatments, such as quenching, annealing and temperature jump, etc., have been studied extensively[8-14] at atmospheric pressure. In addition to a phenomenological description of kinetic ageing, other theoretical considerations, based on statistical mechanics using a hole diffusion process model[15] and a stochastic model[16,17], have been proposed to explain the mechanism of kinetics at the molecular level. In this study, investigations have been made to determine the combined effects of thermal and pressure treatments on the glass transition and the relaxation. The basic kinetic equations and the expression for the relaxation time are modified to be both temperature- and pressure-dependent. Theoretical predictions from the general solution of these equations are then compared with the experimental results for a polyurethane elastomer (Solithane 113, $T_g=-20°\mathrm{C}$). Young's modulus has been chosen as the parameter in monitoring the ageing process. It was found that the structural recovery of elastomeric glass is strongly path-dependent on the P–V–T space. A multi-ordering-parameter model can be used to distinguish one glass from another at the same pressure and temperature but with different pressure–temperature history.

FUNDAMENTALS

Thermodynamic considerations

As shown previously[5], in the P–V–T space, the rubbery or liquid state of an amorphous polymer, usually regarded as in equilibrium, can be represented by a liquid (L) surface, of which the differential equation takes the form:

$$\mathrm{d}V_L=V_L\alpha_L(P,T)\mathrm{d}T-V_L\beta_L(P,T)\mathrm{d}P \qquad (1)$$

---

* On leave from China Textile University, Shanghai, People's Republic of China

0032-3861/88/030410–08$03.00
© 1988 Butterworth & Co. (Publishers) Ltd.

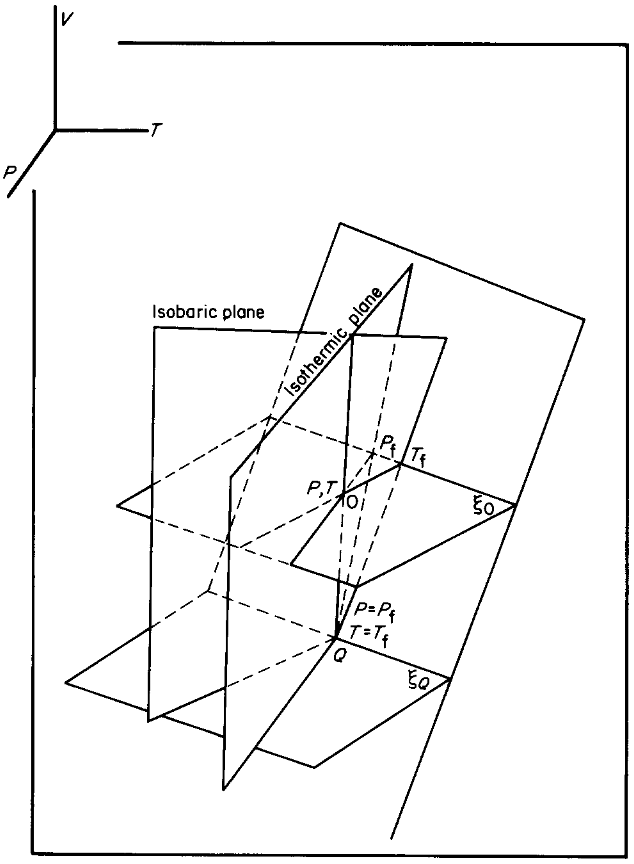

Figure 1 Interrelation between P_f, T_f, T and P on schematic of P–V–T space

On the other hand, glasses (G), in a non-equilibrium state, must be identified with another parameter ξ_i besides T and P, so that the variation of volume of a glass is described by:

$$dV_G = V_G\alpha_G(P,T)dT - V_G\beta_G(P,T)dP + \left(\frac{\partial V_G}{\partial \xi_i}\right)_{P,T} d\xi_i \tag{2}$$

For constant values of ξ_i, i.e. $d\xi_i=0$, there should be a family of iso-ξ_i surfaces, each representing a specified glass. A glass specified by P, T and ξ_i will continuously reduce its volume by increasing ξ_i towards the equilibrium surface during ageing at given P and T, signifying a consecutive variation from one specified glass to another.

The volume change $(\partial V_G/\partial \xi_i)_{P,T}d\xi_i$, responsible for the relaxation, can be shown[5] to be equal to $V\Delta\alpha dT_f$ by introducing the concept of fictive temperature, T_f, referring to the P–V–T space (*Figure 1*). A similar concept, namely, fictive pressure, P_f, can be introduced, and we can then establish the following relation:

$$\left(\frac{\partial V_G}{\partial \xi_i}\right)_{PmT} d\xi_i = V\Delta\alpha dT_f = -V\Delta\beta dP_f \tag{3}$$

Figure 1 illustrates the relationship between V, P, T, P_f and T_f. The point O, which is on the ξ_0 plane[5], specifies the current volume. By drawing an isobaric plane through O (see *Figure 1*) and locating the intersection point of three planes, i.e. the ξ_0 plane, isobaric plane and liquid plane, the fictive temperature T_f is obtained. A similar procedure with the ξ_0 plane, isothermic plane and liquid plane determines the fictive pressure P_f. The fictive temperature T_f and fictive pressure P_f coincide at point Q, which represents the equilibrium. Usually the liquid surface may not be a plane, since $\Delta\alpha$ and $\Delta\beta$, or α_L and β_L, are not constants, as shown by *Table 1*.

Kinetic considerations

Basic equation. The kinetics of the physical ageing phenomenon is conventionally delineated by relative departure from equilibrium, using a dimensionless parameter, $\delta=(V-V_\infty)/V_\infty$, for an isobaric process[8,11]. Furthermore, it can be extended to include variation of both T and P.

The multi-ordering-parameter model, proposed by Kovacs *et al.*[8] and then developed by many others[9–14], partitions δ into a number of sub-elements such that

$$\delta = \sum_{i=1}^{N} \delta_i \tag{4}$$

The variation of each individual δ_i with time, under the concomitant heating rate q and pressurizing rate p, should be governed by distinct differential equations:

$$d\delta_i/dt = -\delta_i/\tau_i - \Delta\alpha_i q + \Delta\beta_i p \qquad i=1,2\ldots,N \tag{5}$$

where $\Delta\alpha_i(P,T)$ and $\Delta\beta_i(P,T)$ are the difference in thermal expansivity and compressibility, respectively, between the liquid and glassy states of the ith element and τ_i is the corresponding relaxation time.

Summing up the solutions of the distinct equations (5), in the limit of large N, with initial conditions given, we obtain the basic equation governing the volume relaxation as:

$$\delta(t) = \delta_0\phi(t,t_0) - \int_{t_0}^{t} [\Delta\alpha(P,T)q(t') - \Delta\beta(P,T)p(t')]\phi(t,t')dt' \tag{6}$$

where $\Delta\alpha$ and $\Delta\beta$ are functions of P and T, whereas $q(t)=dT/dt$ and $p(t)=dP/dt$ are the prescribed thermal and pressure treatment history. The Williams–Watt[18] function is employed for evaluating the response function ϕ in (6):

$$\phi(t,t') = \exp\left[-\left(\int_{t'}^{t} \frac{dt''}{\tau(T(t''),P(t''),T_f(t''))}\right)^{\beta}\right] \tag{7}$$

in which, near the transition where $\Delta\beta$ and $\Delta\alpha$ do not vary substantially, T, T_f, P and P_f can be mutually converted by the relation:

$$\delta = \Delta\alpha(T_f - T) = \Delta\beta(P - P_f) \tag{8}$$

Table 1 Physical constants of Solithane 113

P (kbar)	T_α (K)	$\Delta\alpha$ ($K^{-1} \times 10^4$)	$\Delta\beta$ ($kbar^{-1}$)	$\Delta\beta/\Delta\alpha$ ($K\,kbar^{-1}$)	dT_α/dP ($K\,kbar^{-1}$)
0	275	4.9	1.80	37	18
1	292	2.8	0.78	28	15
2	305	2.4	0.53	22	12
3	316	1.7	0.29	17	11
4	326	1.3	–	–	10.5

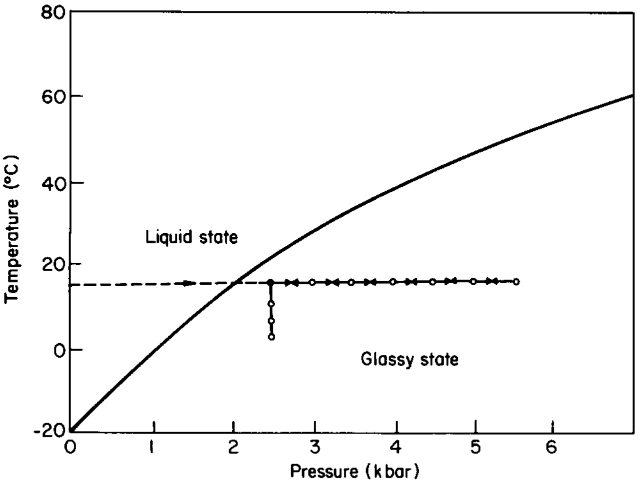

Figure 2 Pressure vs. transition temperature for Solithane 113

At points (P,T) far away from the transition, the differential of (8) gives

$$\begin{aligned} d\delta &= \Delta\alpha(T_f,P)dT_f - \Delta\alpha(T,P)dT \\ &= \Delta\beta(T,P)dP - \Delta\beta(T,P_f)dP_f \end{aligned} \qquad (9)$$

The integral forms of (9) for an isotherm and isobar are, respectively, shown to be:

$$\begin{aligned} (\Delta\delta)_T &= \int_{P_0}^{P} \Delta\beta(T,x)\,dx - \int_{P_{f_0}}^{P_f} \Delta\beta(T,y)\,dy \\ (\Delta\delta)_P &= \int_{T_{f_0}}^{T_f} \Delta\alpha(x,P)\,dx - \int_{T_0}^{T} \Delta\alpha(y,P)\,dy \end{aligned} \qquad (10)$$

Relaxation time. In this work, the relaxation time τ depends on T, P and δ. When the pressure is atmospheric pressure, we set $P=0$ and the Arrhenius equation is expressed as[19,20]:

$$\tau = A\exp\left(\frac{xE_a}{RT} + \frac{(1-x)E_a}{RT_f}\right) \qquad (11)$$

When glasses are formed at different but constant pressures with the same cooling rate, crossing their respective T_g, the relaxation time for each glass should take the same value, i.e. $(\tau)_{P_i} = \text{constant}$[21]. Moreover, at the transition temperature, $T = T_f = T_g$, the following relation should hold:

$$\frac{E_{a(P)}}{RT_g(P)} = \left(\frac{E_a}{RT_g}\right)_{\text{atm}} \qquad (12)$$

Therefore, $E_{a,P}$ may be expressed as:

$$E_{a(P)} = E_a[T_g(P)/T_g] = E_a[1 + (b/a)P + (c/a)P^2 + \ldots] \qquad (13)$$

in which $E_{a(P)}$ and E_a are the activation energies near equilibrium under pressure P and atmospheric pressure, respectively. The pressure dependence of the glass transition temperature, $T_g(P)$, can be expressed for a general glass[5] transition line in *Figure 2* as:

$$T_g(P) = a + bP + cP^2 + \ldots \qquad (14)$$

For Solithane 113 (in appropriate units):

$$a = T_g = 253, \qquad b = 19, \qquad c = -1.265$$

Tool's expression[19] for the relaxation time $\tau(T,\delta)$ at atmospheric pressure is:

$$\tau(T,\delta) = \tau_r a_\delta a_T \qquad (15)$$

where τ_r is the reference relaxation time at T_r at equilibrium, and a_T and a_δ are shift factors, which may be obtained by use of (11) as:

$$a_T = \frac{\tau(T,0)}{\tau(T_r,0)} = \exp\left(\frac{E_a}{R}(T^{-1} - T_r^{-1})\right) = \exp\left(\frac{E_a}{RTT_r}(T_r - T)\right)$$

$$\begin{aligned} a_\delta = \frac{\tau(T,\delta)}{\tau(T,0)} &= \exp\left((1-x)\frac{E_a}{RTT_f}(T - T_f)\right) \\ &= \exp\left(-(1-x)\frac{E_a}{RTT_f}\frac{\delta}{\Delta\alpha}\right) \end{aligned}$$

Instead of attempting to use a new shift factor a_P in addition to a_δ and a_T, we express $\tau(T,P,\delta)$ in terms of P in the following manner:

$$\tau(T,P,\delta) = \tau_r a_\delta(P) a_T(P) \qquad (16)$$

where

$$a_T(P) = \exp\left(\frac{E_a(P)}{RTT_r(P)}[T_r(P) - T]\right)$$

$$a_\delta(P) = \exp\left((1-x)\frac{E_a(P)}{RTT_f}(T - T_f)\right)$$

Equation (13) still holds for $E_{a(P)}$ in the above expressions. As long as the reference relaxation time τ_r is assigned a unique value at each pressure, the corresponding $T_r(P)$ has to conform to the following relation as a result of (11) at equilibrium:

$$\left(\frac{E_a}{RT_r}\right)_{\text{atm}} = \frac{E_a(P)}{RT_r(P)} \qquad (17)$$

This leads to the same relation at $T_g(P)$, i.e.

$$T_r(P) = T_r[1 + (b/a)P + (c/a)P^2] \qquad (18)$$

We have determined that the theoretical calculations could not predict the memory effect (see section on 'Memory behaviour'), for which the structural recovery gave rise to a broad δ peak as a function of ageing time. The calculated half-width of the peak is too narrow to coincide with the experimental data. To broaden the peaks of the theoretical curves, we varied the model constants in (11), of which x proved most effective. However, a broader peak beyond the range $0 < x < 1$ was still required. Therefore, we have further modified (11) by separating apparent activation energies into two parts, one for the temperature and the other for the structure dependence as:

$$\tau = A\exp\left(\frac{xE_a}{RT} + \frac{(1-x)E_s}{RT_f}\right) \qquad (19)$$

where E_s is a function of $\delta = \Delta\alpha(T_f - T)$, indicative of structure dependence. Since (19) should reduce to the simple Arrhenius expression on the liquid line, where $T_f = T$, E_s must be a positive function approaching E_a when $T = T_f$, i.e.

$$\begin{gathered} E_s = E_s(T_f, T) > 0 \\ E_s(T_f, T_f) = E_s(T, T) = E_a \end{gathered} \qquad (20)$$

Thus, a simple relationship can be adopted between E_a and E_s as

$$E_s = E_a\left(1 - \frac{B}{T}(T_f - T)\right) = E_a\left(1 - \frac{B}{T}\frac{\delta}{\Delta\alpha}\right) \qquad (21)$$

implying that the activation energy contributed by the structure increases when the glass relaxes towards equilibrium, i.e. δ decreasing and approaching zero as a limit. B is a material constant expressed as a proportionality function of x. Henceforth

$$a_\delta(P) = \frac{\tau(T,P,\delta)}{\tau(T,P,0)} = \exp\left[-(1-x)\frac{E_a(P)}{R}\left(\frac{1+B}{TT_f}\right)(T_f - T)\right] \qquad (22)$$

If we choose $B = 2x/(1-x)$, then (22) takes the following form:

$$a_\delta(P) = \exp\left(-(1+x)\frac{E_a(P)}{RTT_f}(T_f - T)\right) \qquad (23)$$

which can predict the wide range of memory effects observed in our experiment.

CALCULATIONS PERTAINING TO ISOTHERMAL AND ISOBARIC RESPONSES NEAR THE TRANSITION

Setting $p = 0$ or $q = 0$ in (6) and then utilizing the response function (7) in which the expression for the relaxation time (16) and the conversion relation (9) are employed, isobaric and isothermal processes (T_f vs. T and P_f vs. P) can be described by the following equations:

for an isobar at P,

$$\begin{gathered} T_f = T + (T_{f0} - T_0)\phi(T,T_0) - \int_{T_0}^{T}\phi(T,T')\mathrm{d}T' \\ \phi(T,T') = \exp\left[-\left(\frac{1}{q}\int_{T'}^{T}\frac{\mathrm{d}T''}{\tau[T(t''),P,T_f(t'')]}\right)^{\beta}\right] \end{gathered} \qquad (24)$$

for an isotherm at T,

$$\begin{gathered} P_f = P + (P_{f0} - P_0)\phi(P,P_0) - \int_{P_0}^{P}\phi(P,P')\mathrm{d}P' \\ \phi(P,P') = \exp\left[-\left(\frac{1}{P}\int_{P'}^{P}\frac{\mathrm{d}P''}{\tau[T,P(t''),T_f(t'')]}\right)^{\beta}\right] \end{gathered} \qquad (25)$$

where

$$T_f(t'') = T + [P(t'') - P_f(t'')]\left(\frac{\Delta\beta}{\Delta\alpha}\right)_{P(t'')}$$

For Solithane 113, the numerical calculations performed throughout this paper are based on the model constants:

$$\Theta = E_a/RT_r^2 = 0.51 \text{ (ref. 22)}, \qquad x = 0.35$$

$$\beta = 0.25, \qquad T_r = 263\,\mathrm{K}, \qquad \tau_r = 1\,\mathrm{min}$$

and the functional forms of $\Delta\beta(P)$ and $\Delta\alpha(P)$ were obtained by interpolating the values given in *Table 1*[22].

Figure 3 displays the temperature dependence of calculated fictive temperature at various pressures, $P = 0$, 1, 2, 3 kbar with cooling rate $q = -0.02°\mathrm{C\,min^{-1}}$. Each curve shows a transition region through which substantial departure of T_f from T can be observed. As the temperature decreases, but before T_g is reached, T_f of the polymer in the liquid state is equal to T. The T_g under these pressures (*Figure 2*, full curve) are respectively 253, 273, 283 and 294 K, which are located somewhere at the beginning of the transition region. A rectangular rule was used for numerical integration with $\Delta T = 0.1$. The inadequacy caused by such a step length should be tolerable[11]. *Figure 4* shows the pressure dependence of calculated fictive pressure at various temperatures, namely $T = 273$, 283 and 294 K, corresponding respectively to $P_g = 1$, 2, 3 kbar in which an equivalent pressurizing rate $p = 0.0019\,\mathrm{kbar\,min^{-1}}$ was used. As the pressure increases, but before P_g is reached, P_f of the polymer in the liquid state is equal to P. The equivalent pressurizing rate is defined as $p = -q\Delta\alpha/\Delta\beta$, obtained by

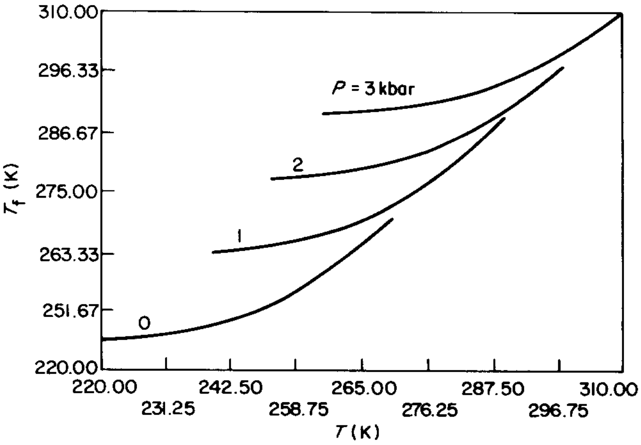

Figure 3 Temperature dependence of calculated fictive temperature at various pressures

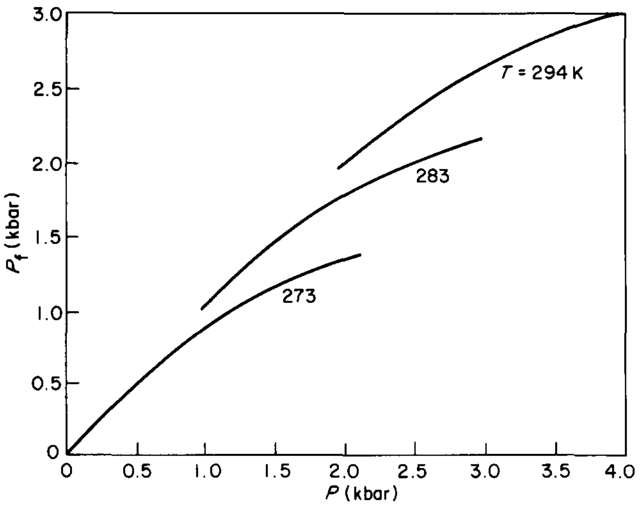

Figure 4 Pressure dependence of calculated fictive pressure at various temperatures

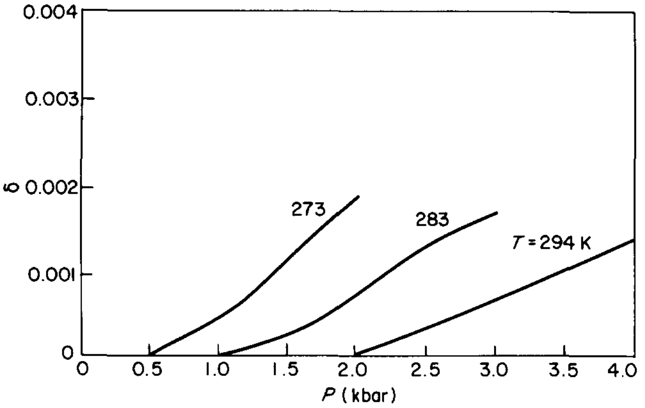

Figure 5 Pressure vs. variation of δ along isotherms

equating $\Delta\alpha q$ to $-\Delta\beta p$ in (6), implying comparable timescales of observation for an isobar with q and an isotherm with p. *Figure 5* illustrates the variation of δ in terms of pressure along these isotherms. Direct comparison of T and P scans (*Figures 3* and *4*), which is made possible by a purely kinetic consideration incorporating the three-dimensional space scheme (*Figure 1*), demonstrates their correspondence to each other near the glass transition. The two scans differ in that the isobaric glass relaxes more slowly during cooling below T_f than the isothermic glass during pressurizing above P_f. That is, T_f from the P scan in the glass region decreases less sharply than P_f in the T scan increases. The T_f or P_f would remain constant if the relaxation ceases completely.

PHYSICAL AGEING OF GLASSES FORMED BY DIFFERENT P–T PATHS

Elastomeric glasses of Solithane 113 formed via either isobaric or isothermal paths were studied at various states of pressure and temperature for their ageing behaviour in this high-pressure laboratory[23,24]. Young's moduli (E) were measured at various intervals of ageing to monitor the variation of δ through a relation:

$$\delta = A(P,T)\left(\frac{1}{E(t)} - \frac{1}{E_\infty(P,T)}\right) \qquad (26)$$

where $E(t)$ is the instantaneous Young's modulus measured at ageing time t, $E_\infty(P,T)$ is the equilibrium Young's modulus and A is the proportionality function to be determined from experimental data of the ageing at (T,P) of a special glass formed along a prescribed path.

Theoretical calculations, based on the general solution of the multi-ordering-parameter, equation (6), and response function, equation (5), have to be coupled with the conversion relation

$$\mathrm{d}\delta = \Delta\beta(P)\mathrm{d}P - \Delta\beta(P_f)\mathrm{d}P_f = \Delta\alpha(T_f)\mathrm{d}T_f$$

for an isothermal path, or

$$\mathrm{d}\delta = -\Delta\beta(P_f)\mathrm{d}P_f = \Delta\alpha(T_f)\mathrm{d}T_f - \Delta\alpha(T)\mathrm{d}T$$

for an isobaric path. In *Figures 6* and *7*, δ is plotted against time for each glass formed by first lowering temperature along an isobar ($P = 0$) respectively to different temperatures, viz. 15, 4.5, −6.5, −25°C, at $q = -0.5$°C min^{-1} and then applying pressure to 3 kbar at a rate $p = 0.25$ kbar min^{-1} along the isotherms. The data points, which were converted from the E measurement[24], begin 1 h after ageing starts. The δ *versus* ageing time curves for glasses formed by first applying pressure to 3 kbar along the 35°C isotherm, then lowering temperature respectively for each glass to the desired level, viz. 15, 4.5, −6.5 and −25°C, along the 3 kbar isobar at

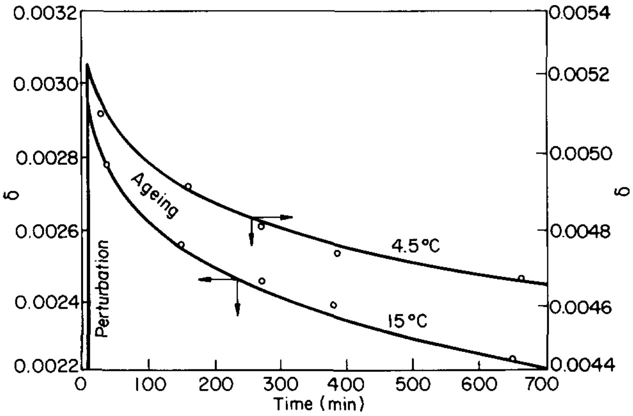

Figure 6 δ vs. time for the treatment of glasses along prescribed paths (isotherms)

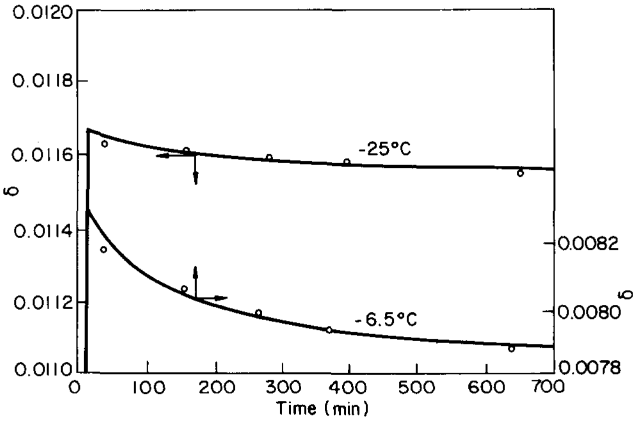

Figure 7 δ vs. time for the treatment of glasses along prescribed paths (isotherms)

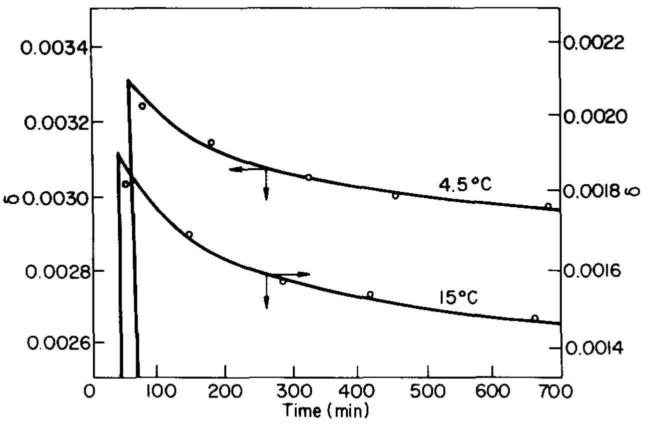

Figure 8 δ vs. time for the treatment of glasses along prescribed paths (isobars)

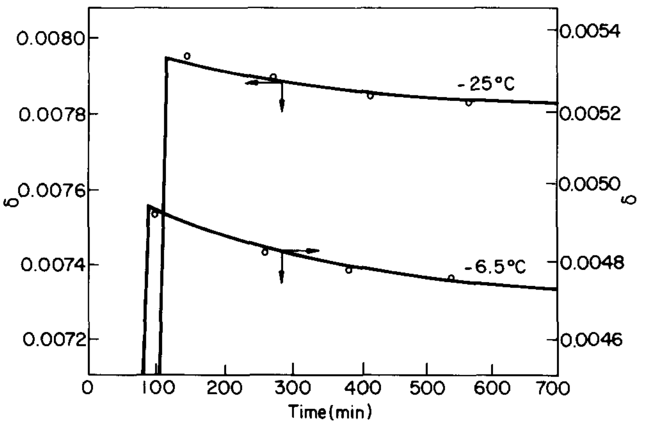

Figure 9 δ vs. time for the treatment of glasses along prescribed paths (isobars)

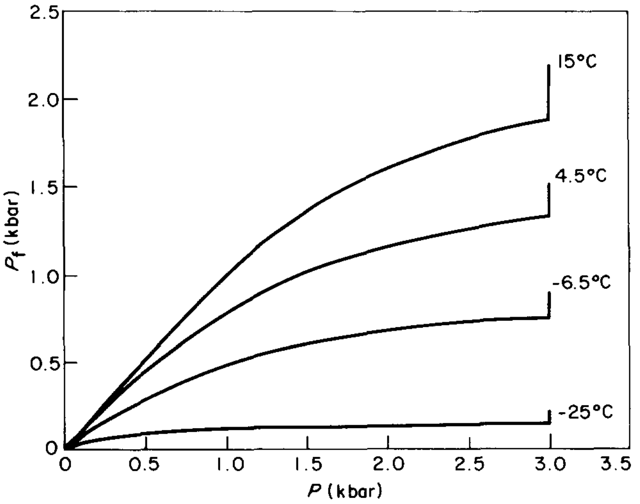

Figure 10 P_f vs. P for isotherms on *Figures 6* and *7*

the same p and q are shown in *Figures 8* and *9*. It is observed from these curves that the higher the temperature of ageing, the lower is δ (*Figures 6* and *7*) because the glass is closer to the equilibrium temperature (18°C at 3 kbar), and that the higher the temperature, the faster is the relaxation as revealed by the steeper slope of the curves (*Figures 8* and *9*) because the relaxation time is shorter at higher temperatures. *Figure 10* shows P_f vs. P for the isotherms. Each curve has a transition zone before 3.0 kbar is reached except at −25°C which is already below the glass transition temperature under 0 kbar.

MEMORY BEHAVIOUR

The memory effect associated with two consecutive temperature perturbations at reasonably slow rates of cooling and heating has been studied extensively by many investigators$^{8-14}$. In the present work, calculations were made to predict the memory behaviour of Solithane 113 subject to pressure and temperature perturbations. The experimental procedure was as follows:

(1) The original glass (the control sample) was formed by pressurizing Solithane to 2.5 kbar with $p = 0.25$ kbar min^{-1} at 15°C as shown in *Figure 2*.

(2) The control sample was immediately given a pressure perturbation, $\Delta P = 0.5$ kbar, that is pressured to 3 kbar (step 1).

(3) The sample was then aged at 3 kbar for 10 h (step 2).

(4) The pressure was reduced back to 2.5 kbar at $p = -0.5$ kbar min^{-1} (step 3).

(5) The sample was allowed to undergo relaxation at 2.5 kbar and 15°C, the Young's modulus measured at various ageing times (step 4) and δ obtained.

(6) The same procedure was followed with $\Delta P = 1.5$ kbar and $\Delta P = 2$ kbar.

The resulting δ exhibits a peak due to memory effect by the pressure perturbation as shown in *Figures 11* and *12*.

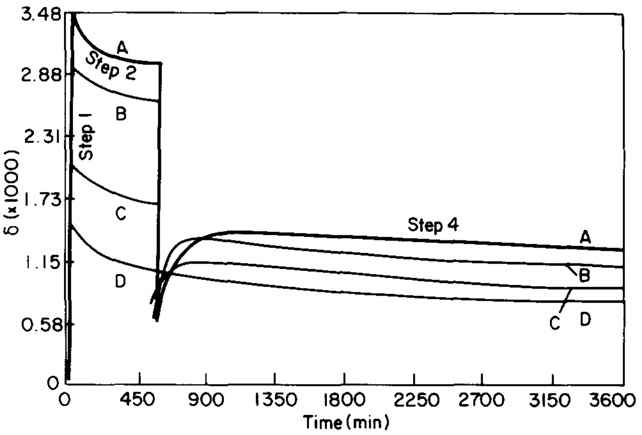

Figure 11 Theoretical results of isotherms with memory effect due to pressure perturbations

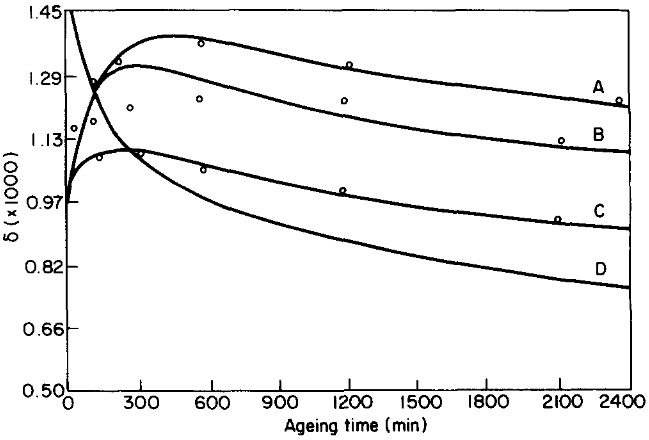

Figure 12 Memory effect, δ vs. ageing time (step 4 of *Figure 11*)

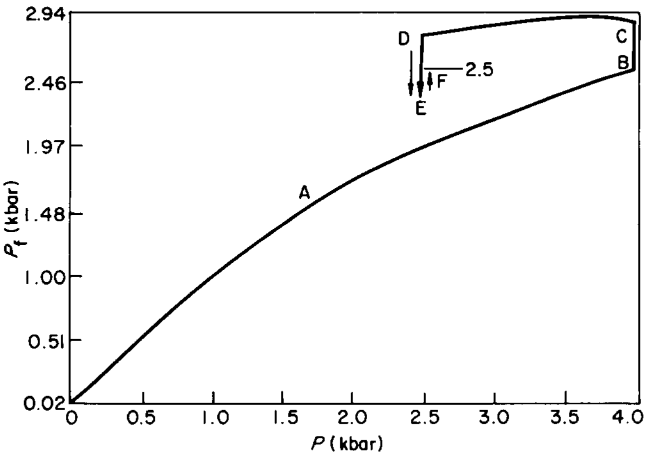

Figure 13 P_f vs. P for curve B of *Figure 11*

Equation (16) modified to include these four steps with initial condition $\delta_0 = 0$ ($P_0 \doteq P_{f0}$) at t_0, can be written as:

$$\delta(t) = p_1 \int_{t_0}^{t} \Delta\beta(t')\phi(t,t')\mathrm{d}t' \qquad (28a)$$

where $t_0 \leqslant t < t_1$ (step 1),

$$\delta(t) = p_1 \int_{t_0}^{t_1} \Delta\beta(t')\phi(t,t')\mathrm{d}t' \qquad (28b)$$

where $t_1 \leqslant t < t_2$ (step 2),

$$\delta(t) = p_1 \int_{t_0}^{t_1} \Delta\beta(t')\phi(t,t')\mathrm{d}t' + p_2 \int_{t_2}^{t} \Delta\beta(t')\phi(t,t')\mathrm{d}t' \qquad (28c)$$

where $t_2 \leqslant t < t_3$ and p is zero between t_1 and t_2 (step 3),

$$\delta(t) = p_1 \int_{t_0}^{t_1} \Delta\beta(t')\phi(t,t')\mathrm{d}t' + p_2 \int_{t_2}^{t_3} \Delta\beta(t')\phi(t,t')\mathrm{d}t' \qquad (28d)$$

where $t_3 \leqslant t$ (step 4).

The results of these isotherms are shown by the curves A, B and C ($\Delta p = 2.0$, 1.5 and 0.5 kbar) in *Figure 11*, together with curve D which shows the relaxation behaviour of the control sample, that is relaxation of the original glass at 2.5 kbar and 15°C without pressure perturbation. These curves are reproduced in *Figure 12* without steps 1 to 3 in order to compare with the experimental data. *Figure 13* shows how P_f changes during the pressure perturbation cycle. As pressure is increased from atmospheric to 4 kbar, P_f increases from 0 to B, crossing A where T_g occurs; P_f increases from B to C, while P is held constant for 10 h and P_f undergoes a change from C to D by first increasing slightly and then decreasing during depressurization from 4 to 2.5 kbar. The ageing at 2.5 kbar and 15°C is represented by P_f going from D to E to F but never reaching 2.5 kbar. The detail of changes of P_f during the ageing process (D to E to F in *Figure 13*) is plotted against ageing time in *Figure 14*.

In temperature perturbation experiments, the samples were initially pressurized to 2.5 kbar at 15°C. Without waiting at that state, they were cooled down immediately to 10, 5 and 0°C respectively, held at those temperatures for 10 h, heated back to 15°C and allowed to age, and tested for elastic response at various ageing times. The rates of heating and cooling during the process were 0.5°C min^{-1} (q_2) and -1.0°C min (q_1) respectively. The basic equation for the above process may be written as:

$$\delta(t) = p_1 \int_{t_0}^{t} \Delta\beta(t')\phi(t,t')\mathrm{d}t' \qquad (29a)$$

where $t_0 \leqslant t < t_1$

$$\delta(t) = p_1 \int_{t_0}^{t_1} \Delta\beta(t')\phi(t,t')\mathrm{d}t' - q_1 \int_{t_1}^{t} \Delta\alpha(t')\phi(t,t')\mathrm{d}t \qquad (29b)$$

where $t_1 \leqslant t < t_2$,

$$\delta(t) = p_1 \int_{t_0}^{t_1} \Delta\beta(t')\phi(t,t')\mathrm{d}t' - q_1 \int_{t_1}^{t_2} \Delta\alpha(t')\phi(t,t')\mathrm{d}t' \qquad (29c)$$

where $t_2 \leqslant t < t_3$,

$$\delta(t) = p_1 \int_{t_0}^{t_1} \Delta\beta(t')\phi(t,t')\mathrm{d}t - q_1 \int_{t_1}^{t_2} \Delta\alpha(t')\phi(t,t')\mathrm{d}t' - q_2 \int_{t_3}^{t} \Delta\alpha(t')\phi(t,t')\mathrm{d}t' \qquad (29d)$$

where $t_3 \leqslant t < t_4$,

$$\delta(t) = p_1 \int_{t_0}^{t_1} \Delta\beta(t')\phi(t,t')\mathrm{d}t' - q_1 \int_{t_1}^{t_2} \Delta\alpha(t')\phi(t,t')\mathrm{d}t' - q_2 \int_{t_3}^{t} \Delta\alpha(t')\phi(t,t')\mathrm{d}t' \qquad (29e)$$

where $t_4 \leqslant t$.

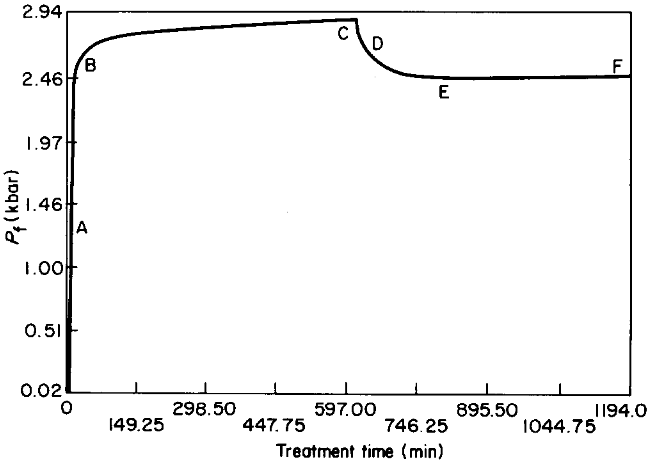

Figure 14 P_f vs. time for curve B of *Figure 11*

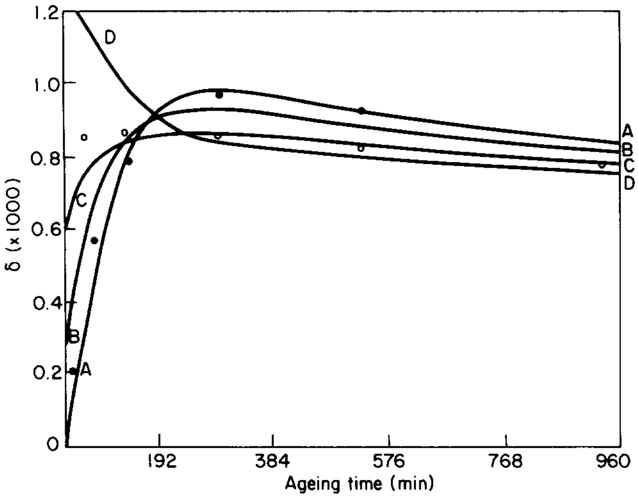

Figure 15 Memory effect, δ vs. ageing time

The results of the above calculations for the memory effect, i.e. δ *versus* ageing time $(t - t_4)$, are plotted in *Figure 15*. The calculated curves agree reasonably well with experimental data[24].

ACKNOWLEDGEMENT

The authors gratefully acknowledge the Propulsion and Energetics Program of the Office of Naval Research (Contract No. N00014-82-K-0608) for its financial support of this research study.

REFERENCES

1 Gibbs, J. H. and DiMarzio, E. A. *J. Chem. Phys.* 1958, **28**, 373
2 DiMarzio, E. A. and Gibbs, J. H. *J. Chem. Phys.* 1958, **28**, 807
3 DiMarzio, E. A., Gibbs, J. H., Fleming, P. D. III and Sanchez, I. C. *Macromolecules* 1976, **9**, 736
4 Adam, G. and Gibbs, J. H. *J. Chem. Phys.* 1965, **43**, 139
5 Pae, K. D., Tang, C.-L. and Shin, E.-S. *J. Appl. Phys.* 1984, **56**, 2426
6 Pae, K. D., Tang, C.-L. and Vijayan, K. *J. Mater. Sci.* in press
7 Rehage, G. *J. Macromol. Sci.–Phys. B* 1980, **18**, 423
8 Kovacs, A. J., Aklonis, J. J., Hutchinson, J. M. and Ramos, A. R. *J. Polym. Sci., Polym. Phys. Edn.* 1974, **17**, 1097
9 Chow, T. S. *Polym. Eng. Sci.* 1984, **24**, 1079
10 Chow, T. S. *J. Polym. Sci., Polym. Phys. Edn.* 1984, **22**, 699
11 Chow, T. S. and Prest, W. M. *J. Appl. Phys.* 1982, **53**, 6568
12 Matsuoka, S. *Polym. Eng. Sci.* 1981, **21**, 907
13 Matsuoka, S., Williams, G., Johnson, G. E., Anderson, E. W. and Kurukawa, T. *Macromolecules* 1985, **18**, 2652
14 Hodge, I. M. *Macromolecules* 1985, **18**, 1980
15 Curro, J. G., Lagasse, R. R. and Simha, R. *Macromolecules* 1982, **15**, 1621
16 Robertson, R. E., Simha, R. and Curro, J. G. *Macromolecules* 1984, **17**, 911
17 Robertson, R. E. *Macromolecules* 1985, **18**, 953
18 Williams, G. and Watt, D. C. *Trans. Faraday Soc.* 1970, **66**, 80; 1971, **67**, 1323
19 Tool, J. *J. Am. Ceram. Soc.* 1946, **29**, 240
20 Narayanaswamy, O. S. *J. Am. Ceram. Soc.* 1971, **54**, 491
21 Havliček, I., Ilavský, M. and Hrouz, J. *J. Macromol. Sci.–Phys. B* 1982, **21**(3), 425
22 Pae, K. D. and Questad, D. L. *J. Polym. Sci., Polym. Phys. Edn.* 1983, **21**, 1195
23 Pae, K. D., Vijayan, K. and Tang, C.-L. Proc. Sixth Int. Conf. Deform., Yield and Fracture Polym., Cambridge, England, 1985, p. 3.1
24 Vijayan, K., Tang, C.-L. and Pae, K. D. *Polymer* 1988, **29**, 396